

# Simulation Calculation of the Magnetic Torque of Dual Mode Permanent Magnet Transmission Based on Magnetic Circuit Analysis

ZHENGYAO ZOU<sup>1,2</sup> AND YING LIU<sup>1</sup>

<sup>1</sup>College of Electronic and Mechanical Engineering, Nanjing Forestry University, Nanjing 210037, China

<sup>2</sup>School of Mechatronic Engineering, Jinling Institute of Technology, Nanjing 211169, China

Corresponding author: Ying Liu (lying\_new@163.com)

This work was supported by the Jinling Institute of Science and Technology High-Level Talent Research Start-Up Project (jit-rcyj-201701).

**ABSTRACT** A method of cutting permanent magnets with circular arcs of offset center was proposed on the basis of the principle of similarity under the condition of slip drive to obtain a permanent magnet transmission scheme for low permanent magnet torque fluctuations. The magnetic flux distribution of each region in the magnetic circuit was altered by changing the shape of the permanent magnet. Different magnetic torque curves were obtained by selecting silicon steel sheet with different thicknesses. The relationship between the magnetic flux distribution and the relative rotation angle in the silicon steel sheet was further analyzed, and the direct cause of the influence of the thickness of the silicon steel sheet on the magnetic torque was obtained. The parameters of different eccentric arcs were selected for simulation calculation, and a smooth magnetic torque curve was obtained after fixing the thickness of the silicon steel sheet. On the basis of the results of the former two, the parameters of the eccentric arc were obtained by the magnetic torque value volatility using an approximation method, and the magnetic torque value was measured by making the physical object. According to the results of the simulation and experiment, the permanent magnets with eccentric arcs can be used to obtain the smooth magnetic torque in the range of a  $0^{\circ}$ – $90^{\circ}$  relative rotation angle, which has a certain application value.

**INDEX TERMS** Dual mode permanent magnet transmission, magnetic flux distribution, silicon steel sheet's thickness, eccentric arc's parameters, simulation calculation, experimental verification.

## I. INTRODUCTION

The magnetic transmission concepts dated back to the early 20th century [1]. Recently, many studies on permanent magnet transmission have emerged. The axial-flux modulated superconducting magnetic gear has currently been specifically studied using a superconducting bulk magnet replacing conventional permanent magnet [2]. The coaxial magnetic gear with an eccentric pole of the inner rotor and Halbach arrays of the outer rotor was proposed and studied to improve the torque density of a coaxial magnetic gear (CMG) [3]. Substantial studies on the CMG were performed in [4]–[6]. Magnetic gears that were well suited to execute high-torque direct-drive operations for oceanic wave energy harvesting applications were designed [7]. The shape of the flux modulators of the concentric magnetic gear affects the torque capability and ripples [8]. A new geometry was proposed for the

magnetic gear to reduce the eddy-current loss of permanent magnets and improve the torque transfer efficiency [9]. The permanent magnet shape is one of the main factors affecting the performance of permanent magnet transmission. The CMG has a great advantage when a large radius and a small axial length are permissible. Hence, the CMG is suitable for the drivetrain of vehicles [10]. A novel topology of a planetary magnetic gear having only two rotating parts demonstrated a torque density of  $187 \text{ kN} \cdot \text{m}/\text{m}^3$  [11]. The air-gap magnetic fields and eddy-current densities of a non-rotary mechanical flux adjuster (MFA) were investigated under the different shifting distances of a MFA, which reveals the fairly good torque regulation effects [12]. The designed electromagnetic coupling regulator controller can ensure the stable voltage export by changing the magnitude and direction of the excitation current to adjust the size of the air gap magnetic field. Therefore, the problem of output voltage instability in the wide speed and load ranges of the hybrid excitation generator was solved [13]. A novel structure of a HP

The associate editor coordinating the review of this manuscript and approving it for publication was Jenny Mahoney.

motor was proposed to simplify the manufacturing processes and increase the efficiency [14]. A new analysis method of the permanent magnet irreversible demagnetization was proposed, which uses the dynamic air-gap flux density simulated under various temperature B–H curves and the relationship between the braking torques, to predict the demagnetization of the permanent magnet [15]. A verification process was conducted. In a considerably wide range of slip speeds, the torques were predicted by the presented method match well with those obtained by the three-dimensional finite element analysis and experimental measurement [16]. When the slip speed between the two disks is 0.2, the temperature of the copper is up to 200 °, and the PM is 30 °. The temperature rise of the permanent magnet is small, but the temperature of the copper is high [17]. A multiphase hybrid permanent magnet generator for series hybrid electric vehicles was designed, which includes two rotor elements: a permanent magnet and a wound field rotor with a 30% split ratio, coupled on the same shaft in one machine housing [18].

However, the current scheme of permanent magnet transmission is difficult to apply in automotive power transmission because it cannot perform high efficiency in constant variable transmission [19], [20]. The magnitude and direction of torques, which are exerted on the inner rotor while keeping the ring and the outer rotor fixed, are periodically changing [21]. This scenario is not very suitable for slip transmission. A continuously variable transmission can best match the engine and the entire vehicle, but the expected increase in fuel economy and acceleration performance has not been achieved in many cases [22]. Attempts to increase the efficiency of the conventional planetary gear-type automatic transmission with a torque converter have been made through increasing the number of gears and lockup clutches [23]. It is very complex. The dual-clutch transmission leads the seamless output torque during a shift, when considerable heat is generated due to friction, by disengaging the off-going clutch simultaneously as engaging the oncoming clutch [24]. If a permanent magnet slip drive with high torque density exists, then it will be able to meet this demand and consist of few components. Several calculate methods to the torque of the magnetic device were researched and proved viable by the test experiment [25]. The maximum torque of the improved prototype magnetic gear dramatically increased, which is similar to a conventional planetary type mechanical gear [26]. Given the existence of the slip, the eddy current coupling the maximum efficiency is lower than 97%, while its ratio can be variable [27]. To obtain a smooth magnetic torque as designing a permanent magnet motor, research was carried out using a special-shaped permanent magnet, and the experimental verification was obtained [28]. The switched reluctance motor under a heavy load has local magnetic saturation, which is rationally utilized to accurately estimate the speed and position [29]. A novel device with a variable ratio and a high torque density was designed to best match the engine and the entire vehicle [30]. The calculation and analysis of magnetic fields are commonly used in two laws,

namely, the *Ampère circuital theorem* and *flux continuity principle* [31]. For magnetic circuit analysis, the magnetic law is the Ohm law, that is, the magneto motive force acting on the magnetic circuit is equal to that in the magnetic circuit. The magnetic flux is multiplied by the magnetic resistance, which is similar to the Ohm law in the circuit, and the magnetic circuit of the mechanism in the silicon steel sheet changes, which has a great influence on the law of magnetic torques [32]. If a mechanism can integrate the advantages of permanent magnet and eddy current couplings, then it can realize efficient transmission and continuous variable transmission. Hence, it can widen the range of the permanent magnet transmission application. When the automobile transmission shifts due to the speed ratio change of the transmission, the driving and load speeds are inconsistent, a transition phase to make the driving and load speeds consistent occurs. In this transitional phase, if the transmission torque value is simply reduced and the power is not interrupted, then the slip mechanism applies, and the comfort of the occupant improves. Further reducing the fluctuation of the transmission torque value during the transition phase can improve the comfort of the occupant. Given its use in automobiles, the mechanism is demanding in terms of small size, light weight, high transmission efficiency, reliable operation, and simple maintenance. The design difficulty of this mechanism type is how to obtain the change of the magnetic torque value when the slip drive is small. To address this challenge, this study focuses on how to obtain the small fluctuation magnetic torque of the active part and the follower of the magnetic drive within a relative rotation angle of 90 ° (hereinafter referred to as the relative rotation angle). When operating in the slip drive mode, if the relative angle exceeds 90 degrees, the direction of the magnetic torque between the drive and output disks changes, which is not conducive to smooth transmission. Therefore, dividing the slip drive into small transmission time units is necessary. In each unit, the drive disk was rotated back and forth with respect to the output disk, and the relative rotation angle is at most 90 degrees. The direction and magnitude of the magnetic torque transmitted in the relative angular range are required to be constant to achieve the smooth transmission of the mechanism.

## II. STRUCTURE AND WORKING PRINCIPLE

The designed mechanism is installed between the engine and the transmission. It can realize the slip-and-drive and coupling modes. When the transmitter shifts, the mechanism works at the slip-and-drive mode: the drive disk is connected to the engine through a drive control mechanism, and the output disk receives the input power through non-contact magnetic field force. Two fan-shaped permanent magnets are uniformly arranged on the input disk, and two shaped permanent magnets are uniformly arranged on the output disk to reach a small fluctuation in torque value under the slip-and-drive duct. Fig. 1 shows the structure of the mechanism and the distribution of permanent magnets. The mechanism working at slip-and-drive mode as the clutch release,

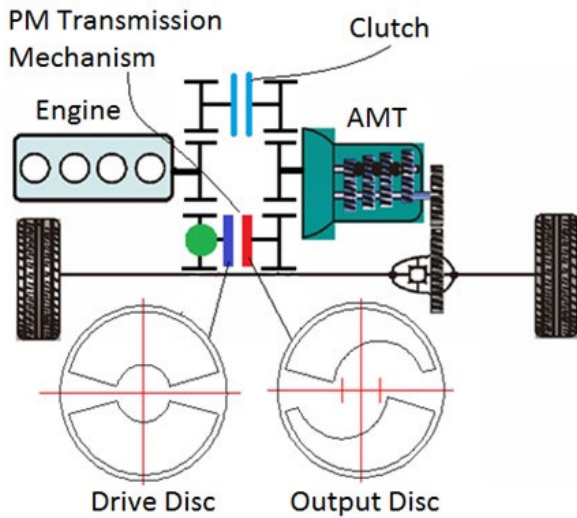


FIGURE 1. System structure and distribution of permanent magnets.

the mechanism uses the non-contact characteristics of magnetic field force to realize the continuously variable shifting function. If the constant input speed is higher than the varying output speed, then the gear ratio can be continuously changed within a range. The time of the mechanism working at slip-and-drive mode is divided into several similar small periods of time and the each small period is divided into two parts. During the first part, the drive disk receives the input energy to drive the output disk. It releases its own kinetic energy to drive the output disk during the second half part. The drive disk is frequently accelerated and decelerated in each unit. Therefore, a control system capable of frequently absorbing energy is needed, which can absorb and release input energy at a high frequency and adapt to the acceleration and deceleration conditions of the drive disk.

III. EFFECT OF PERMANENT MAGNET SHAPE ON MAGNETIC TORQUE

Fig. 2 shows the established simulation model. The driving and output disks contain 20 pieces of silicon steel sheets, each of whose thickness is 0.5 mm. Two fan-shaped permanent magnets are respectively mounted on the opposite sides of the silicon steel sheet. If the sector magnets are arranged side by side, then the rule that its torques vary with the relative rotation angle is similar to that of sinusoidal curve, which are not suitable for the slip transmission. The shape and size of the permanent magnets on the drive and output magnetic disks are initially designed as a regular sector with an outer diameter of 130 mm, an inner diameter of 46 mm, and a sector angle of 150°. The interval angle between the magnets on the same magnetic disk is initially designed to be 30°. In the simulation software, the permanent magnet material is Nd-Fe-B (named Neodymium Iron Boron:48/11), and the residual flux density (Br) is 1039.67 mT (20°). The outer material is selected from silicon steel sheet, which has the high magnetic permeability (named M-36 26 Ga). The thickness of air gap is 2 mm. The rotational speed of the driving magnetic disk

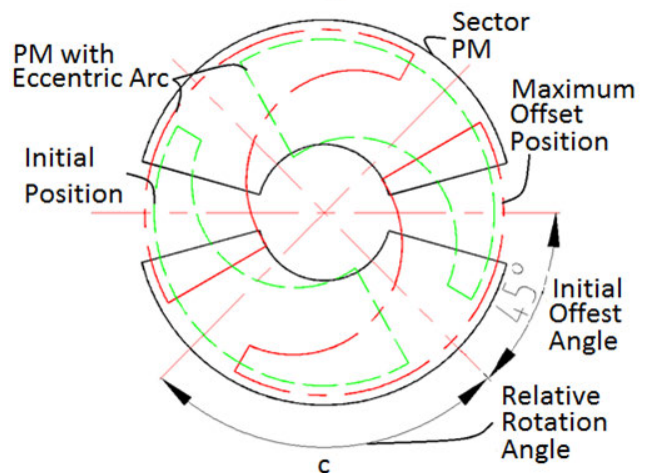
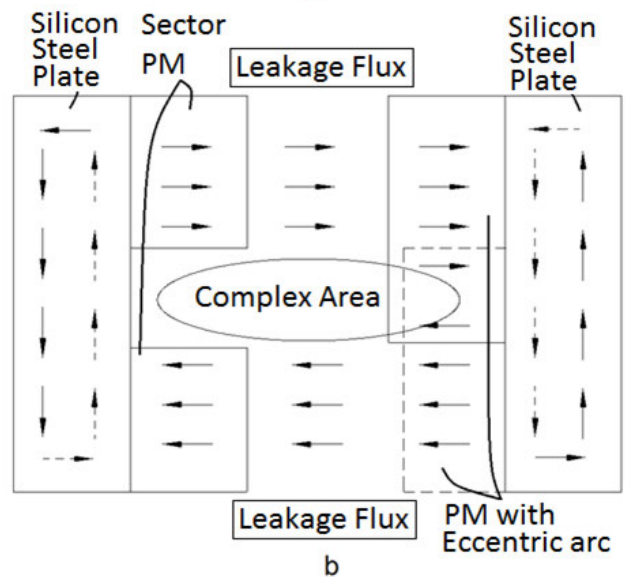
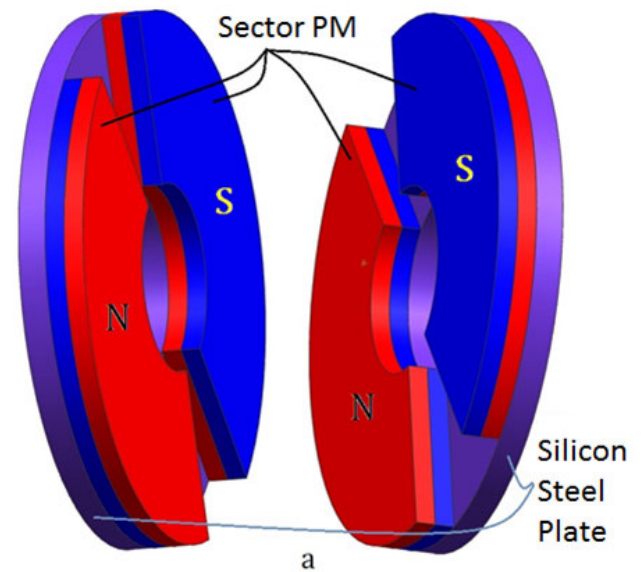


FIGURE 2. a. Established simulation model. b. Equivalent magnetic circuit. c. Parameters on a relative rotation angle.

is set to 1°/ms, and the time of simulation is set to be 360 ms. Accordingly, the driving magnetic disk will rotate

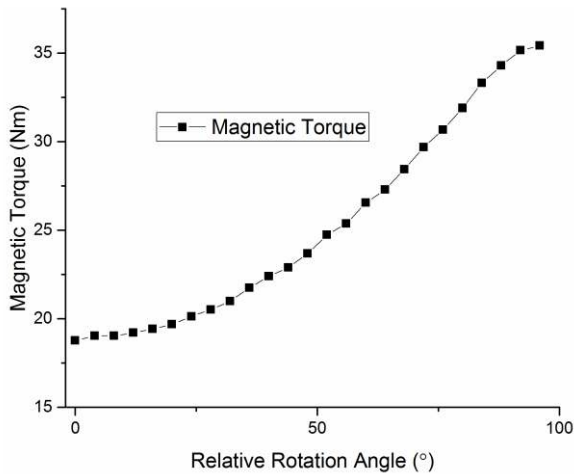


FIGURE 3. Simulation value of torque of sector-shaped permanent magnet.

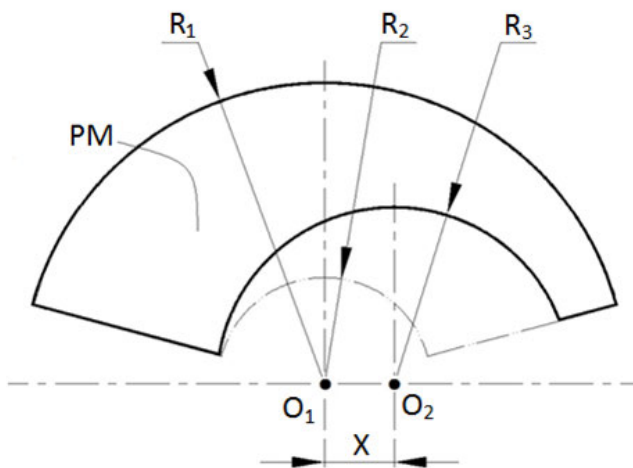
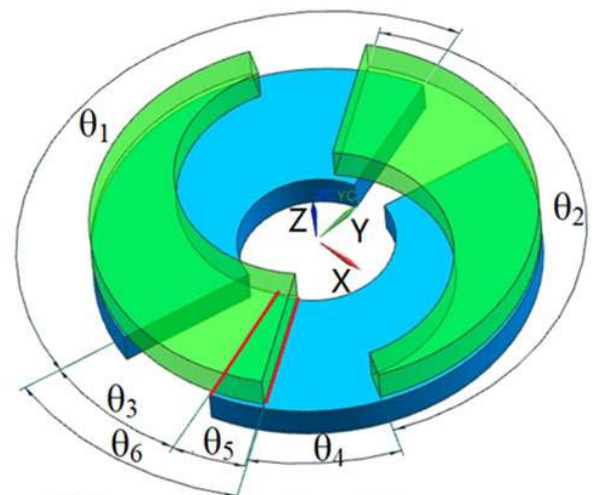


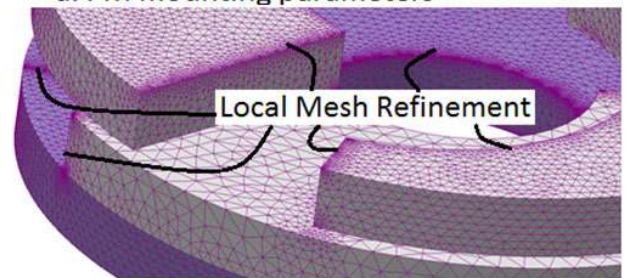
FIGURE 4. Permanent magnet with eccentric arc.

for 360 ° relative to output magnetic disk in 360 ms. The simulation result segment with a length of 90 ms is selected as the research object. The equivalent magnetic circuit and the parameters depending on relative rotation angle are provided.

When the PMs installed on the drive and output magnetic disks are fan-shaped, the torque characteristics of the moving disk simulated by MAGNET software are shown in Fig. 3 (20 °). The value of magnetic torques changed greatly corresponding to the relative rotation angle between 0 and 90°. The magnetic torque does not vary smoothly within the range of relative rotate angle between 0° and 90°. The magnetic torque varies greatly within the range of relative rotate angle between 30° and 95° and triggers large vibrations when the device is operating in the slip drive mode. Having observed the variation of the torque curve, the research envisages the use of arc-cut sector-shaped PMs to obtain a smooth magnetic torque characteristic solution according to the principle of similarity. A section between the start and end angles was selected as the object of study. The larger the magnetic field force radius is, the larger the magnetic torque value is; otherwise, the smaller the magnetic



a. PM mounting parameters



b. The local mesh refinement model

FIGURE 5. Permanent magnet fixed parameters and 3D finite element model.

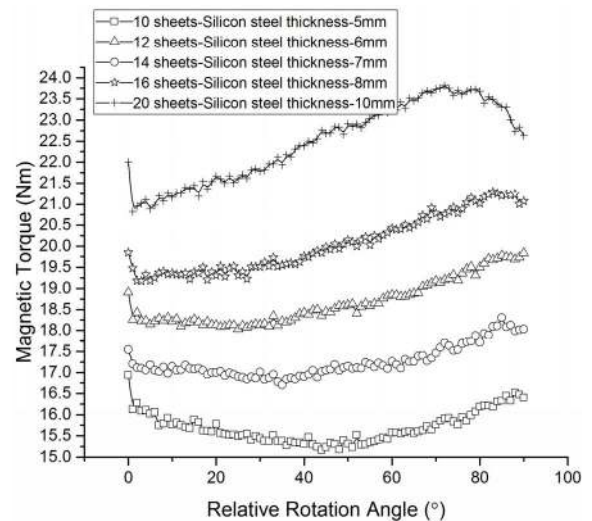


FIGURE 6. Magnetic torque-relative rotation angle curve corresponding to the different thicknesses of silicon steel sheets.

torque value is. It is considered to reduce the PM from the part that has a small radius of the sector magnet. The mean value of the magnetic torque must be steady when the driving, and adding weight is unnecessary.

Many methods are available to obtain the smooth curve of the output torque. In our solution, we change the shape of

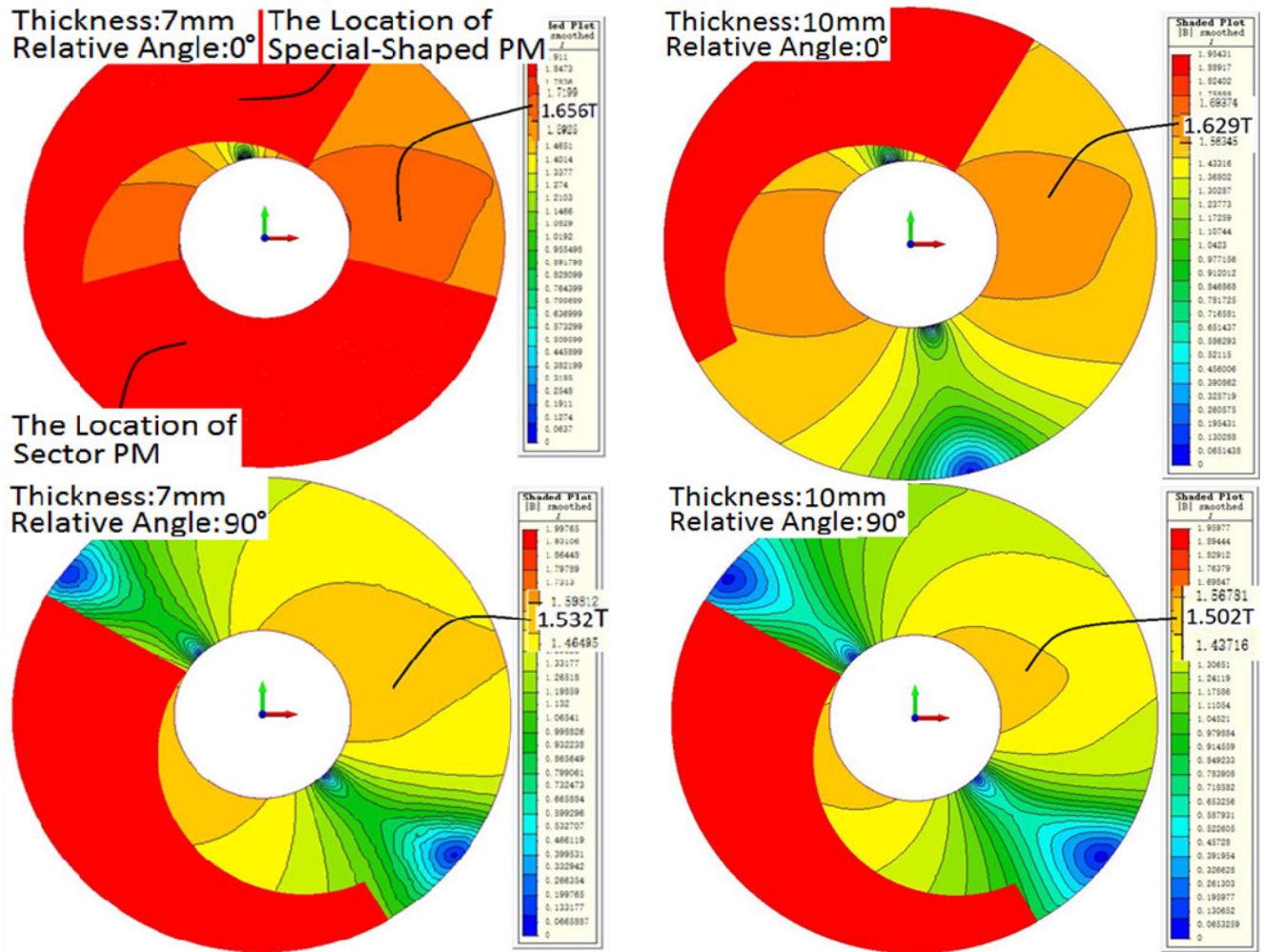


FIGURE 7. Distribution of the magnetic flux density in the different parts of the silicon steel sheet.

the PM in the output disk to adapt to the special case of the magnetic circuit change to obtain the stable magnetic torque Fig.4 exhibits that  $O_1$  refers to the center of the sector-shaped PM,  $R_2$  refers to the inner diameters, and  $R_1$  refers to the outer ones. The center (In Fig. 4, it is represented by  $O_2$ ) of the eccentric circular arc is  $(x, 0)$ , and the radius  $R_3$  is  $|x| + R_2$ . Hence gaining the adjustment parameters is easy when cutting. The parameters are also easier to adjust. Many parameters affect the shape of the output magnetic torque. Some parameters are fixed, and then  $x$  and  $R_3$  are selected for this research to obtain a magnetic torque shape with small fluctuations. Finally, the proposed method in our research is proven to be one of the ways to solve the problem. The arc itself is a quadratic curve, the right half of the PM is cut off, and the dimension of the remaining portion of the PM in the radial direction changes as the law of the quadratic curve along the central angle.

Fig. 5 shows the relative initial position of the PM and the 3D finite element model and the arrangement of the PMs ( $\theta_1 = 150^\circ, \theta_2 = 150^\circ, \theta_3 = 30^\circ, \theta_4 = 30^\circ, \theta_5 = 15^\circ, \theta_6 = 45^\circ$ ). The special-shaped PMs are mounted

on the output disk, while the fan-shaped PMs are mounted on the driving disk. Under the slip drive mode, the drive disk rotates in relative to outputs disk in  $-z$  direction  $90^\circ$  and then rotates in the  $+Z$  direction. The local meshes were refined to improve the accuracy of simulation calculations. The driving and output disks contain several pieces of silicon steel sheets, each of whose thickness is 0.5 mm (Fig. 2 shows the location of the silicon steel sheet). The magnetic field diagram of the device is very complicated. The direction of magnetic flux lines in the PM and the silicon steel plate varied greatly as the relative rotation angle changed. An additional sub-figure is added to show the key relative positions of the magnetic direction flux line corresponding to 0 and 90 degrees.

The torque curve is shown in Fig.6, where the thickness of the sector-shaped and special-shaped PMs is 10 mm, the thickness of the air layer is 2 mm, the  $X$  is 14 mm, and the temperature is  $20^\circ$ . When the thickness of the silicon steel sheet is 10 mm, the magnetic torque value is large. When the value of relative rotation angle is between  $70^\circ$  to  $90^\circ$ , the values of magnet torques and relative angles are negatively correlated. Hence, changing the value of  $X$

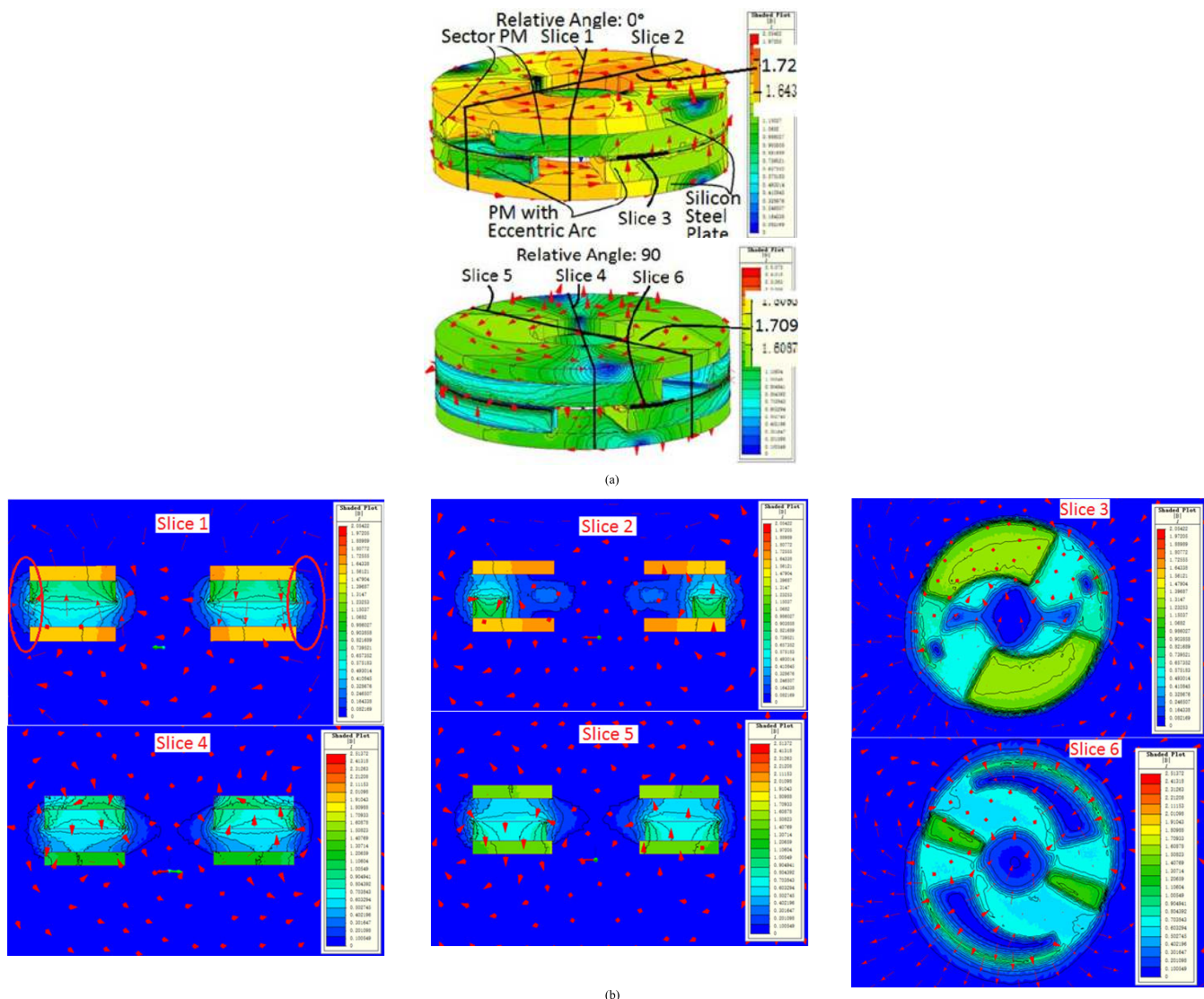


FIGURE 8. a. The magnetic flux lines of the model. b. Magnetic flux lines in different parts.

to obtain a smooth magnetic torque curve is not conducive, especially in the range of relative angles of  $80^\circ$  to  $90^\circ$ . When the thickness of the silicon steel sheet is 5 mm, the magnetic torque value first decreases as the relative rotation angle increases and then increases. It is also not conducive to obtaining a smooth magnetic torque curve by changing the  $X$  value, and the magnetic torque value is greatly reduced. After several attempts, the model with a silicon steel sheet thickness of 7 mm is selected, where the average magnetic torque value was moderate and the PM parameter can be further optimized to obtain a stable magnetic torque curve.

Changing the number of silicon steel sheets, that is, changing the total thickness of the silicon steel plate, can change the curve of the magnetic torque. The reason is that the change of the magnetic flux density in different parts of the silicon steel sheet affects the reluctance of the magnetic circuit and the distribution of the magnetic flux of each branch. The static magnetic field analysis was carried out by selecting a model

with a silicon steel plate with a thickness of 7 mm (14 sheets) and 10 mm (20 sheets), respectively. The change in magnetic flux density in the outermost silicon steel sheet can be seen in Fig. 7 (the silicon steel sheet is 7 mm thick, and the relative rotation angle is  $0^\circ$ ), where magnetic saturation does not occur. For the exploration of the law of obtaining smooth magnetic torques, the distribution of magnetic flux and field lines in key areas are specifically studied. The relative rotation angles of 0 degrees and 90 degrees were selected for the study to simplify the problem and fully explain the problem. Three slices were selected for each location for the analysis and the magnetic field conditions at the corresponding two locations were compared. In the axial direction, the strength of the outer magnetic field of the silicon steel sheet is small, and the outer side of the radial direction has a slightly strong magnetic field distribution. Therefore, providing a house for magnetic field shielding depending on the magnetic field distribution is necessary. Fig. 8 (a, b) shows the magnetic flux

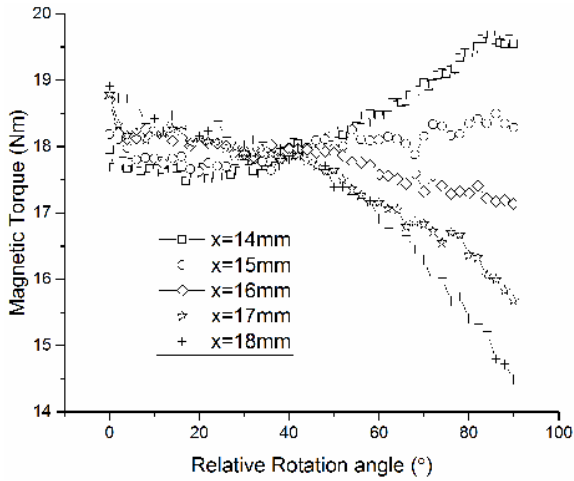


FIGURE 9. Magnetic torque-relative rotation angle curve corresponding to the different X.

lines and the distribution changing of magnetic flux density between the drive and output disks. They are the main factors that affect the smoothness of the magnetic torque. When the relative rotation angle is  $90^\circ$ , no region where the magnetic flux is saturated in the outermost silicon steel sheet emerges. Accordingly, obtaining the smooth curve of magnetic torques becomes easy by changing the value of X when the thickness of the silicon steel sheet is 7 mm. Therefore, the silicon steel sheet and the PM must be precisely installed to prevent the deviation of the relative position of the silicon steel sheet or the position between the silicon steel sheet and the PM at different relative angles, which would trigger the dramatically large deviation of the actual measured magnetic torque value and simulation calculation in some relative angle segments.

With the reasonable shape of the PM and thickness of the silicon steel sheet selected, the simulated magnetic torque curve is obtained by changing the value of X. Take the x value (Table 1), and use the MAGNET<sup>®</sup> software to simulate calculate after trial cutting. The law under the simulation calculation is shown in Fig. 9, where the temperature is 20 degrees. The five X values are selected, and the torque characteristics obtained by simulation are shown in Fig. 9. The torque characteristic is the most smooth when  $X = 15$ . The torque curve when  $X = 15$  has convex attribute, which lays the foundation for further optimization.

IV. RESULTS AND ANALYSIS

The simulation results reveal that if the inner diameter of the PM is 46 mm and the outer diameter is 130 mm, then low torque ripples can be obtained at a relative rotation angle in the range of  $[0^\circ, 90^\circ]$  where the x value is 15.8 mm and the radius of the cutting circle, the eccentric arc, is 38.8 mm. The prototype machine can be seen in the Fig. 10, which is manufactured by the above parameters. Two curved grooves on the output disk and two pins on the drive disk are available. Under the action of magnetic torques, the initial positions of the output and drive disks are determined by pins and curved grooves.

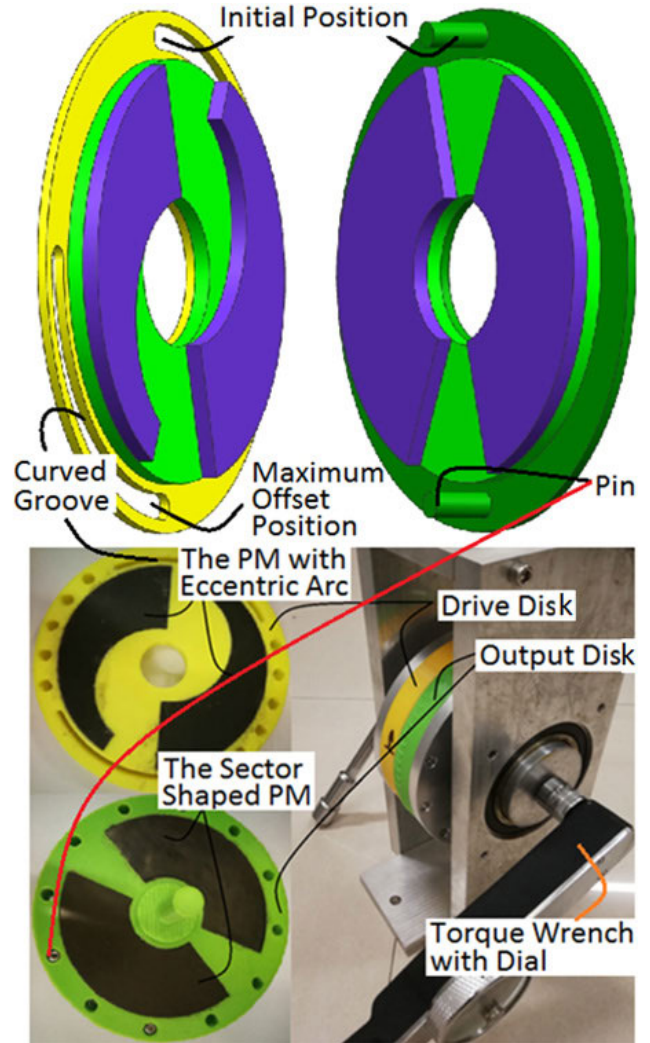
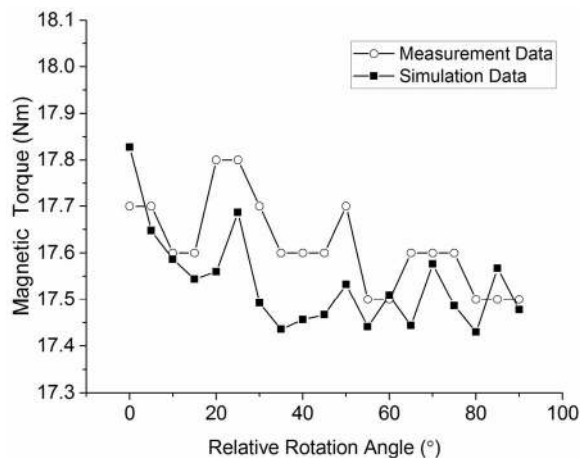


FIGURE 10. Experimental device for testing.

The maximum relative rotation angle corresponds to the maximum offset position. The disk holder is made of PLA materials by using a 3D printer, and an angle scale is printed on the outer circle to facilitate measurement and improve measurement accuracy. The metal disk is behind the plastic disk to improve the overall rigidity of the disk tray. The machine installed only the moving and output disks (the air gap between the two disks is 2 mm) to measure the magnetic torque value of the relative rotation angle in the range of  $[0^\circ, 90^\circ]$ . We would like to introduce the detailed testing procedure as follows. The output disk is fixed, and the drive disk is rotated with respect to the output disk by a torque wrench. During the testing process, the magnetic torque value would be recorded every 5 degrees, and the temperature is 20 degrees. The torque is measured three times by a dial torque wrench (the minimum scale is 0.5 Nm). The minimum scale of torque wrench with dial is 0.5 Nm, which affects the reading accuracy. Fig. 11 shows that the average torque of the machine is 17.6158 Nm, the minimum value is 17.5 Nm, the maximum value is 17.8 Nm, the standard deviation is 0.0958 Nm, and that the maximum deviation from the average



**FIGURE 11.** The magnetic torque value of optimized simulation calculation and measured magnetic torque value.

is 1.05%. The simulation model with the same parameters has a torque of an average value of 17.5162 Nm, a minimum value of 17.5352 Nm, a maximum value of 17.8276 Nm, a standard deviation of 0.1012 Nm, and a maximum deviation from an average of 1.78%. The software calculation accuracy is set to 1%. Therefore, a torque law with less volatility can be obtained in terms of the model parameters. Evidently, the PM cutting method and simulation results are reasonable.

The silicon steel sheets and PMs in the experimental system must be reliably fixed to prevent abnormal changes in the magnetic torque value during measurement. A flat bearing was added between the shaft and the drive and output disks to reduce the abnormal friction torque. Solving this problem is also possible by arranging reasonably the plurality of the sets of the drive and output disks in the axial direction and giving the drive or output disks at both ends a relatively rigid support.

## V. CONCLUSION

Under the condition of fixing the inner diameter, outer diameter, and thickness of the PM, the magnetic circuit structure in this study can acquire low torque ripples within a relative rotation angle (between the drive and output disks) in the range of  $[0^\circ, 90^\circ]$ , making the PM drive mechanism transmit smoothly in the case of the slip drive. The magnetic torque drive transmitted by the moving disk in the case of slip is basically constant, and the fluctuation is small. Therefore, this mechanism has significant advantages in some cases where the output is affected by the input. Subsequent tests further achieve good results by making PMs have consistent performance, optimizing the support of the test mechanism, and using high precision test tools at different temperatures.

The mechanism can work with smooth magnetic torques when working in slip conditions; hence, it can realize the continuous variable transmission as the hydraulic torque converter and the dual-clutch. Compared with the hydraulic torque converter and the dual-clutch, the main components of the mechanism are sector PMs and PM with eccentric arcs,

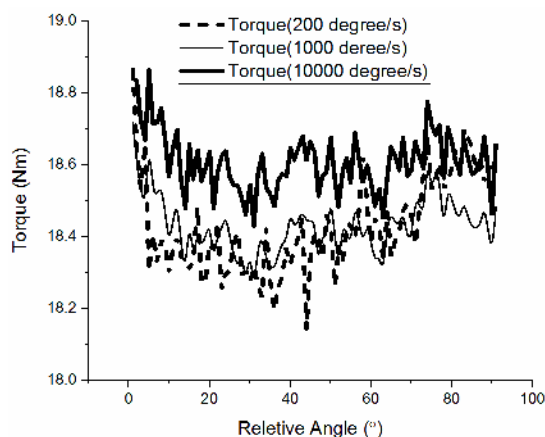


**FIGURE 12.** Magnetic torque-relative rotation angle curve at different relative rotational speeds.

which are very convenient to manufacture by the mold and have low requirements on equipment. The power and torque delivered by the mechanism are related to the relative rotation speed. The transmission efficiency of this mechanism, which is related to the efficiency and relative speed of the control transmission mechanism, can be obtained by the transfer power of the output and drive disks. Studying the effect of a relative rotational speed on magnetic torques, the research finds that the magnetic torque values are unequal with different relative rotation angles when the relative rotational speed is small, but the average magnetic torque values are similar.

Given that the spatial distribution of the silicon steel sheets and the PMs and the current values caused by themselves are different, the magnetic torque curve at the relative rotational speeds of 200 degrees/s and 1000 degrees/s cross each other and have similar average values (Fig. 12). The ohmic loss powers of PM are 0.022, 0.386, and 26.8 W at the speeds of 200, 1000, and 10000 degree/s. The iron loss powers of the silicon steel sheet are 0.019 W, 0.146 W, and 4.803W at the speeds of 200, 1000, and 10000 degree/s. The corresponding mean torques are 18.428 Nm, 18.43 Nm, and 18.609 Nm and the efficiency values are 99.95%, 99.91%, and 99.71%. The power loss of the drive control mechanism was not calculated. Hence, the magnetic torque at a low relative speed can be represented by the static measured magnetic torque by measuring the actual model. When the relative rotational speed is large, that is, when the rotational speed of the drive disk is much higher than that of the output disk, the transmitted magnetic torque value also increases. This slightly increases the efficiency when the difference in rotational speed is large and also has the effect of reducing the rotational speed difference as quickly as possible. Furthermore, it can be used as a closed component of the split transmission to realize the continuously variable transmission of the entire split transmission system.

Presently, the PMs with eccentric arcs have obtained a stationary magnetic moment at a relative rotation angle. The maximum value of relative rotational speed would increase with the ratio of the transmitted magnetic torque value to



the moment of the output disk inertia growing. Studying the influence of the various parameters of the mechanism on the law of magnetic torque value is necessary; hence, several outstanding mechanisms are studied for good practical applications. The development of control mechanisms that can work at high frequencies is the focus of future works.

## REFERENCES

- [1] A. Sardar and S. B. Muttana, "Evolution of transmission for EVs, HEVs; Potential for magnetic transmission," *Auto Tech Rev.*, vol. 21, no. 5, pp. 18–23, May 2013.
- [2] K. Dong, H. Yu, and M. Hu, "Study of an axial-flux modulated superconducting magnetic gear," *IEEE Trans. Appl. Supercond.*, vol. 29, no. 2, Mar. 2019, Art. no. 5000505.
- [3] L. Jing, T. Zhang, Y. Gao, R. Qu, Y. Huang, and T. Ben, "A novel HTS modulated coaxial magnetic gear with eccentric structure and Halbach arrays," *IEEE Trans. Appl. Supercond.*, vol. 29, no. 5, Aug. 2019, Art. no. 5000705.
- [4] M. Johnson, M. C. Gardner, and H. A. Toliyat, "A parameterized linear magnetic equivalent circuit for analysis and design of radial flux magnetic gears—Part II: Evaluation," *IEEE Trans. Energy Convers.*, vol. 33, no. 2, pp. 792–800, Jun. 2018.
- [5] M. Johnson, M. C. Gardner, and H. A. Toliyat, "Design comparison of NdFeB and ferrite radial flux permanent magnet coaxial magnetic gears," *IEEE Trans. Ind. Appl.*, vol. 54, no. 2, pp. 1254–1263, Mar./Apr. 2018.
- [6] Y. Li, H. Lin, Q. Tao, X. Lu, H. Yang, S. Fang, and H. Wang, "Analytical analysis of an adjustable-speed permanent magnet eddy-current coupling with a non-rotary mechanical flux adjuster," *IEEE Trans. Magn.*, vol. 55, no. 6, Jun. 2019, Art. no. 8000805.
- [7] O. Dobzhanskiy, E. Hossain, E. Amiri, R. Gouws, V. Grebenikov, L. Mazurenko, M. Pryjmak, and R. Gamaliia, "Axial-flux PM disk generator with magnetic gear for oceanic wave energy harvesting," *IEEE Access*, vol. 7, pp. 44813–44822, Apr. 2019.
- [8] M. C. Gardner, M. Johnson, and H. A. Toliyat, "Analysis of high gear ratio capabilities for single-stage, series multistage, and compound differential coaxial magnetic gears," *IEEE Trans. Energy Convers.*, vol. 34, no. 2, pp. 665–672, Jun. 2019.
- [9] E.-J. Park, C.-S. Gim, S.-Y. Jung, and Y.-J. Kim, "A gear efficiency improvement in magnetic gear by eddy-current loss reduction," *Int. J. Appl. Electromagn. Mech.*, vol. 60, no. 1, pp. 103–112, Apr. 2019.
- [10] M. C. Gardner, M. Johnson, and H. A. Toliyat, "Comparison of surface permanent magnet axial and radial flux coaxial magnetic gears," *IEEE Trans. Energy Convers.*, vol. 33, no. 4, pp. 2250–2259, Dec. 2018.
- [11] O. Molokanov, P. Dergachev, S. Osipkin, E. Kuznetsova, and P. Kurbatov, "A novel double-rotor planetary magnetic gear," *IEEE Trans. Magn.*, vol. 54, no. 11, Nov. 2018, Art. no. 8107405.
- [12] X. Zhang, Q. Du, J. Xu, Y. Zhao, and S. Ma, "Development and analysis of the magnetic circuit on double-radial permanent magnet and salient-pole electromagnetic hybrid excitation generator for vehicles," *Chin. J. Mech. Eng.*, vol. 32, no. 1, p. 33, Dec. 2019.
- [13] J.-G. Lee, H.-K. Yeo, H.-K. Jung, T.-K. Kim, and J.-S. Ro, "Electromagnetic and thermal analysis and design of a novel-structured surface-mounted permanent magnet motor with high-power-density," *IET Electr. Power Appl.*, vol. 13, no. 4, pp. 472–478, Apr. 2019.
- [14] L. Ye, M. Cao, Y. Liu, and D. Li, "Multi-field coupling analysis and demagnetization experiment of permanent magnet retarder for heavy vehicles (MAY 2018)," *IEEE Access*, vol. 7, pp. 50734–50745, Apr. 2019.
- [15] J. Wang and J. Zhu, "A simple method for performance prediction of permanent magnet eddy current couplings using a new magnetic equivalent circuit model," *IEEE Trans. Ind. Electron.*, vol. 65, no. 3, pp. 2487–2495, Mar. 2018.
- [16] D. Zheng, D. Wang, S. Li, H. Zhang, L. Yu, and Z. Li, "Electromagnetic-thermal model for improved axial-flux eddy current couplings with combine rectangle-shaped magnets," *IEEE Access*, vol. 6, pp. 26383–26390, 2018.
- [17] A. S. Al-Adsani and O. Beik, "Design of a multiphase hybrid permanent magnet generator for series hybrid EV," *IEEE Trans. Energy Convers.*, vol. 33, no. 3, pp. 1499–1507, Sep. 2018.
- [18] H. Chen, X. Liu, J. Zhao, and N. A. O. Demerdash, "Magnetic-coupling characteristics investigation of a dual-rotor fault-tolerant PMSM," *IEEE Trans. Energy Convers.*, vol. 33, no. 1, pp. 362–372, Mar. 2018.
- [19] Y. Ando, M. Ito, and I. Murakami, "Development of cylindrical magnetic gear prototype," *Int. J. Appl. Electromagn. Mech.*, vol. 33, no. 4, pp. 1397–1404, Oct. 2010.
- [20] K. Atallah, S. D. Calverley, and D. Howe, "Design, analysis and realisation of a high-performance magnetic gear," *IEE Proc. Elect. Power Appl.*, vol. 151, no. 2, pp. 135–143, Mar. 2004.
- [21] T. Lubin, S. Mezani, and A. Rezzoug, "Analytical computation of the magnetic field distribution in a magnetic gear," *IEEE Trans. Magn.*, vol. 46, no. 7, pp. 2611–2621, Jul. 2010.
- [22] N. Srivastava and I. Haque, "A review on belt and chain continuously variable transmissions (CVT): Dynamics and control," *Mechanism Mach. Theory.*, vol. 44, no. 1, pp. 19–41, Jan. 2009.
- [23] L. Gaertner and M. Ebenhoch, "The ZF automatic transmission 9HP48 transmission system, design and mechanical parts," *SAE Int. J. Passenger Cars Mech. Syst.*, vol. 6, no. 2, pp. 908–917, Jan. 2013.
- [24] J. J. Oh, J. Kim, and S. B. Choi, "Design of self-energizing clutch actuator for dual-clutch transmission," *IEEE/ASME Trans. Mechatronics.*, vol. 21, no. 2, pp. 795–809, Apr. 2016.
- [25] B. Dolisy, S. Mezani, T. Lubin, and J. Lévêque, "A new analytical torque formula for axial field permanent magnets coupling," *IEEE Trans. Energy Convers.*, vol. 30, no. 3, pp. 892–899, Sep. 2015.
- [26] V. M. Acharya, J. Z. Bird, and M. Calvin, "A flux focusing axial magnetic gear," *IEEE Trans. Magn.*, vol. 49, no. 7, pp. 4092–4095, Jul. 2013.
- [27] X. Y. Xu, *Optimization Theory and Method of Planetary Transmission Mechanism Scheme*. Beijing, China: China Machine Press, 2018.
- [28] J. Wang, H. Lin, S. Fang, and Y. Huang, "A general analytical model of permanent magnet eddy current couplings," *IEEE Trans. Magn.*, vol. 50, no. 1, Jan. 2014, Art. no. 8000109.
- [29] E. Cetin and F. Daldaban, "Analyzing distinctive rotor poles of the axial flux PM motors by using 3D-FEA in view of the magnetic equivalent circuit," *Eng. Sci. Technol. Int. J.*, vol. 20, no. 5, pp. 1421–1429, Oct. 2017.
- [30] Z. Zou, T. Wei, and W. Zou, "Permanent magnet torque converter," U.S. Patent 2016 100 762 926, Apr. 4, 2016.
- [31] B. S. Guru and H. R. Hiziroglu, *Electromagnetic Field Theory Fundamentals*. Beijing, China: China Machine Press, Apr. 2017.
- [32] H. Cai, H. Wang, and M. Li, "Position sensorless control of switched reluctance motors considering the magnetic saturation," *Trans. China Electrotech. Soc.*, vol. 33, no. 12, pp. 2723–2734, Jun. 2018.



**ZHENGYAO ZOU** was born in Danyang, Jiangsu, China, in 1973. He received the B.S. degree in vehicle engineering from Jiangsu University, Zhenjiang, Jiangsu, in 1997, and the M.S. degrees in mechatronic engineering from Southeast University, Nanjing, Jiangsu, in 2007.

He was an Associate Professor (2009) and a Professor (2015) with the Nanjing Institute of Technology. In 2016, he was a Professor with the School of Mechatronic Engineering, Jinling Institute of Technology, Nanjing. He is the author of one book, more than eight articles, and 12 patents. His research interest includes PM transmission technology.



**YING LIU** was born in Nanjing, Jiangsu, China, in 1965. She received the B.S. degree in chemical machinery and equipment from the College of Jiangsu Chemical Technology, Changzhou, Jiangsu, China, in 1988, the M.S. degrees in mechanical manufacture, and the Ph.D. degree in mechanical manufacture and automation from Southeast University, Nanjing, Jiangsu, China, in 1998 and 2006, respectively.

From 1989 to 1999, she was an Engineer with Nanjing Tianjie machinery Limited Company. She was an Associate Professor (2000) and also a Professor (2006) with the College of Mechanical and Electronic Engineering, Nanjing Forestry University, Nanjing. She is currently the Vice Dean of the College of Mechanical and Electronic Engineering. She is the author of one book, more than 70 articles, and eight patents. Her research interests include non-destructive testing, deep learning, and image processing.

Dr. Liu is a member of the China Mechanical Engineering Society and an editorial member of the Journal of Forestry Engineering, China. She was a recipient of the First prize for Educational Achievements from the Jiangsu Provincial Education Department, China, in 2017.

• • •